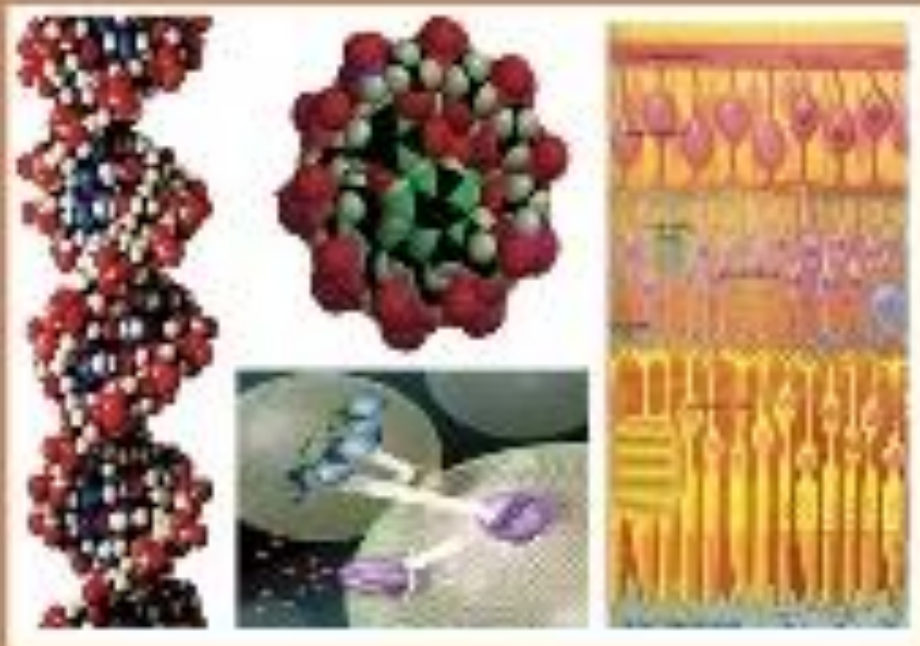




C

EGYPTIAN ACADEMIC JOURNAL OF
BIOLOGICAL SCIENCES
PHYSIOLOGY & MOLECULAR BIOLOGY



ISSN
2090-0767

WWW.EAJBS.ICA.NET

Vol. 15 No. 2 (2023)



Green Synthesis of Silver Nanoparticles from *Penicillium digitatum* Study and Its Effect against *Acinetobacter baumannii* and *Proteus Mirabilis* Bacteria

Wafaa K. Abboud¹, Mahmoud K. S. Al-Jubouri² and Osama N. Nijres³.

¹Department of Biology, College of Education, University of Samarra, Iraq.

²Department of Biology, College of Education, Tikrit University, Iraq.

³Department of Pathological Analysis, University of Samarra, Iraq.

*E-mail: us4010220010@uosamarra.edu.iq

ARTICLE INFO

Article History

Received:9/11/2023

Accepted:11/12/2023

Available:15/12/2023

Keywords:

Greensynthesis.
nanoparticles.
Acinetobacter baumannii, *Proteus mirabilis*,
Penicillium digitatum.

ABSTRACT

Nanoparticle biosynthesis has received increasing attention due to the growing need to develop safe, cost-effective and environmentally friendly technologies biosynthesized for nanomaterials. Therefore, this study aimed to study the effect of silver nanoparticles manufactured from *Penicillium digitatum*, against bacteria and measure the level of interference of antibiotics with nanoparticles. In this paper, silver nanoparticles (Ag NPs) were synthesized using the reduction of the Ag⁺ aqueous ion from *Penicillium digitatum*. The nanoparticles of Ag NPs were also tested by X-ray diffraction and transmission electron microscope (TEM) and UV-visible light absorption spectroscopy method and field-emission scanning electron microscopy (FESEM). Samples is 70 were collected from patients visiting Samarra General Hospital in Samarra city during the period from December 2021 to May 2022 and of both sexes with ages ranging from 1 to 60 years. Samples were collected from different sources of infections, The inhibitory ability of silver nanoparticles produced from mushrooms was studied on pathogenic bacteria, and that was done after making four concentrations, namely 10%, 25%, 50%, and 100% with the control without any concentration of the nanomaterials. The inhibitory activity of silver nanoparticles Ag NPs was tested on some pathogenic bacterial species isolated from burns, wounds, urinary tract and intestinal infections. After that, biochemical tests were performed to diagnose the bacteria, such as the catalase test, the oxidase test, and the urease test, in addition to microscopic examination to confirm the diagnosis by the well diffusion after the sensitivity test was measured. The results showed an inhibitory efficacy of processed silver particles at a concentration of 25, 50, 75 and 100% towards clinical samples for resistance to pathological bacteria *Proteus mirabilis*, *Acinetobacter baumannii*. The role of silver nanoparticles is evident in inhibiting the growth of antibiotic-resistant bacteria, where biologically produced silver nanoparticles can be used as alternatives to antibiotics as the production of nanomaterials is inexpensive and biomaterials are available.

INTRODUCTION

Proteus mirabilis can mostly be found as a living for the gastrointestinal tract of humans and animals. While bacteria are capable of causing a variety of human infections, including wounds, eyes, gastrointestinal tract, and urinary tract. They are mostly observed for urinary tract catheter infections, known as catheter-associated urinary tract infections (Hezam et al., 2023).

This infection is common in long-term catheter patients, such as those residing in nursing homes and chronic care facilities, and may be particularly dangerous for patients with spinal cord injuries. Urinary tract infections (UTIs) and urinary tract infections associated with catheterization, including *Plasmodium pastoralis* are usually complicated by the formation of bladder and kidney stones (urolithiasis) and permanent renal damage and may progress to bacteremia and sepsis. As a matter of fact, catheter-related urinary tract infections are the most common source of bacteremia in nursing homes, and *P. mirabilis* bacteremia occurs more often after urinary tract infection or catheter-related urinary tract infections compared to other sources of infection, bacteremia and sepsis due to *P. mirabilis* carry a high mortality rate. (Al-Ezzy & Algburi, 2023) *P. mirabilis* is a biofilm catheter formation agent, quickly contaminating the surface of the newly inserted urinary catheter. Superficial organelles such as fimbriae and other adhesives seem to play an important role in this process(Al-Halbosiy *et al.*,2017). The enzyme urease also contributes significantly to this process. Urea, our means of eliminating excess nitrogen, is present in high concentrations in the urine, is a urease substrate, and is hydrolyzed into CO₂ and NH₃. The bacterium *Acinetobacter baumannii* has emerged as the main culprit involved in causing hospitalizations, especially in intensive care units (ICUs) worldwide. The ability of this organism to contaminate hospital surfaces for long periods is associated with hospital outbreaks (Hashim *et al.*,2015).The results showed that the ability to infect not only hospitalized patients but also the general population. In hospitals, it gives a mortality rate of 26% up to 43% in intensive care units . *Acinetobacter baumannii* is a major factor of ventilator-related pneumonia, which accounts for about 15% of all hospital-acquired infections, with the highest morbidity and mortality rates in medical wards and especially in intensive care

units. It accounts for about 50% of the total antibiotic use in intensive care units (Gedefie *et al.*, 2021).

In recent years, the proliferation and development of resistance among pathogenic microorganisms, including bacteria, fungi, and viruses, to commonly used antimicrobial agents has resulted in significant health and food-related concerns. Currently, the employment of nanotechnology and nanoparticles (NPs) has been recognized as a novel strategy to address this issue due to their innate antimicrobial properties. Numerous investigations have documented that NPs, encompassing both metal and metal oxide variants, are regarded as a category of substances that merit examination on account of their antimicrobial characteristics (Khezerlou *et al.*, 2018).

Biosynthetic nanoparticles have been used in a variety of applications including drug carriers for targeted delivery, cancer treatment, gene therapy and DNA analysis, antibacterial agents, biosensors, boosting reaction rates, separation science, and magnetic resonance imaging (MRI). (Mittal *et al.*, 2014).

Biological entities and inorganic substances have been in constant contact with each other since the beginning of life on earth. Due to such a regular interaction, life can continue on the planet with well-regulated deposits of minerals. Recently, scientists are interested in the interaction between inorganic molecules and biological species(Hamada *et al.*,2019). Studies have found that many microorganisms can produce inorganic nanoparticles through intracellular or extracellular pathways. Biological methods of nanoparticle synthesis involve the use of living organisms or biological materials to produce nanoparticles. These methods have gained significant interest due to their potential for eco-friendly and sustainable nanoparticle formation as bacteria and fungi have the ability to convert metal ions into nanoparticles by using enzymes or metabolites. (Panacek *et al.*, 2006)

Different microorganisms have

different mechanisms for the formation of nanoparticles. However, Fungi follow methods for the biosynthesis of nanomaterials one of these methods is followed from the top-down, as this method begins with an appreciable size of the material under study and is gradually reduced until the materials arrive to form the nanoscale nanoparticles this method. Metal ions are first confined to the surface or inside the microbial cells. The trapped metal ions are then converted into nanoparticles in the presence of enzymes. The aim of this study identify the ability (biosynthesized) of silver nanoparticle production extracted from *P. digitatum* to have antibacterial activity.(Dahham *et al.*,2019).

MATERIALS AND METHODS

Isolation and Identification of Fungi:

The fungus was isolated from some serotypes of fungi, and then it was cultivated on potato agar at a temperature of 28 °C for 4-7 days. After the growth of the fungal colonies, it was examined microscopically using cotton blue dye. the diagnosis was confirmed molecularly.

Molecular Diagnosis of Fungal Isolates:

The Wizard®Genomic DNA Purification (USA) kit provides a fast and pure way to obtain DNA that can be used in gene amplification using polymerase chain reaction (PCR) technology. The genes were diagnosed in fungal isolates using PCR technology, where the pieces of the gene to be detected were doubled using specialized initiators and through PCR polymerase chain reaction. The primers were prepared in the form of a lyophilized powder (Lyophilized) by Alpha DNA . They were dissolved by adding different volumes of sterile distilled water to obtain a concentration of 10^{-12} of a mole per microliter of distilled water . These prepared concentrations represent the stored solution for each initiator, save this stored solution at a degree of - 20 m and conduct the reaction Final size Al 25 based on what was mentioned (Badali *et al.*,2021).

Preparation of Fungal Biomass and Formation of Silver Nanoparticles:

The fungal mass was prepared by

taking a disc from the growing pure fungal colony using a sterile cork puncture with a diameter of 7 mm. Then the edges of the growing colony are pierced on the fungal growth plate and placed in a conical flask containing 100 ml of potato medium, then placed quietly and carefully so that the disc is on the surface of the medium and left a period of time for the disk to settle on the surface of the medium. It is placed in the incubator at a temperature of 26 C for a period of 5-7 days to obtain the fungal mat . The disc becomes on the surface of the medium and leaves a period of time for the disc to settle on the surface of the medium. It is placed in the incubator at a temperature of 26 m for a period of 5-7 days to obtain the fungal mat (Khashan, *et al.*, 2020). After the formation of the fungal mat, filter the fungal mass using a glass funnel and filter paper (Whatman filter paper No1) and wash well the fungal mass with sterile distilled water three times followed by washing it with deionized water twice to remove the residue of the medium, weighing 20 g of fungi biomass by a sensitive balance and then transferred to glass containers with a capacity of 1000 ml containing 500 ml of deionized water and incubated under the same conditions above with daily shaking by Shaker for 120 hours and after expiry of the specified period. The biomass was leached using filter paper and 0.4 mm filters to obtain the mushroom biomass leachate and collect the leachate and incubation at a temperature of 26 °C and a relative humidity of 75% until use.(Rassin *et al.*,2015).

Preparation of Nano Samples for Examination in The Following Ways:

Absorption of UV Visible Light Spectroscopy:

The sample was prepared for absorption spectrometry 72 hours after placing the solution AgNps in the incubator at 25-26 °C in dark conditions, then 2 ml of the solution AgNps prepared after filtering it from the fungus using sterile filter paper (Whatman filter paper No.1) was taken and shaken well to homogenize the solution and examined with a UV-visible-spectrophotometer after zeroing the device

with sterile distilled water UV-visible-Spectrophotometer from one of the important techniques of detecting nanostructures (Khashan, *et al.*, 2021).

X-Ray Diffraction:

The sample was prepared for testing by converting it into powder by drying method using a hot air oven at a temperature of 60 °C after 72 hours of reaction and after filtering the fungus. The filtered solution was placed in sterile plastic tubes with a volume of 50 ml and placed in a refrigerated centrifuge at a speed of 7000rpm) to flow for 15 minutes and then placed in a hot air oven for 15-20 minutes with constant observation and then Collect the dried precipitate and grind it into a fine powder and prepare approximately 2-3 grams for the purpose of X-RAY examination to determine the granular size.(Hussain *et al.*,2018).

Scanning Electron Microscopy (SEM):

The sample was prepared for diagnosis using scanning electron microscopy SEM to turn it into powder in the same way as the X-ray diffraction test sample.

Field-Emission Scanning Electron Microscopy(FESEM):

The field-emission scanning electron microscope (FESEM) is considered one of the most important tools that can be employed to know the surface topography of materials within the nanoscale, as it allows knowing the shape of nanoparticles with high accuracy and with different magnifications.(Hashim S. S *et al.*,2023).

Antibiotics Sensitivity Test:

Pharmacological susceptibility was tested for 10 types of antibiotics by means of the tablet 5 propagation method, the antibiotics Erythromycin, Ceftraxone, Gentamicin, Amikacin, Azimac, Cefazidime Ampicillin, Ceftaxin, Levofloxacin, Ciprofloxacin, after the bacteria were diagnosed. Pure colonies of the spores under study were transported and the farms were incubated at a temperature of 37 °

C for 15-24 hours . The suspended was diluted using the physiological solution to compare with the standard control sample (McFarland solution) after which the sterile cotton swab was dipped. The bacteria were then spread on the Müller-Henton solid medium in a planning manner more than once and in different directions for the purpose of ensuring that the bacteria to be tested were disseminated at 37 °C for 18 hours for all types of antibiotics .The inhibition diameters were measured in units of measurement (mm) and compared with the standard values.

RESULTS AND DISCUSSION

Microscopic and Molecular Diagnosis of Fungus:

The results of laboratory culture showed that colonies of *Penicillium* appeared after 5 days of incubation at a temperature of 25 °C. shows the microscopic examination of the fungus, which formed dry chains of conidia from brush-shaped conidia, and the conidia ranged from blue to green. DNA sequence analysis SSR indicators were used to detect heterogeneity in the ITS region, which may be due to the length of the piece .The variation in its cytosine and coanin content, thus leading to heterogeneity in the expression of that region (Jillwin *et al.* ,2021 , Swathi,2014). The results obtained from the polymerase chain reaction of this area for both fungi were sent to the Korean company (Macrogen) to determine the similarities and differences between the fungal strains registered in the National Center for Informatics Sciences NCBI. The results of the SSR test revealed that the two fungi under study are new strains with genetic sequences as in Figure (4), and are not registered in the genebank after comparing them with the registered strains of the same sexes as in Figures (1) and (2) . They were registered under the number OR352250 in Iraq and they were named by the researcher as in Figures (1) and (2).


```

GTGATCTTACCGAGTGAGGGCCCTCTGGGTCCAACCTCCCACCCGTGTT
TATTTTACCTTGWTGCTTCGGCGGGCCCGCCTTACTGGCCGCCGGGG
GGCTCACGCTCCCGGGCCCGCGCCCGCGAAGACACCCCGAACTCTG
TCTGAAGATTGCASKCTGAGTGAAAACGAAATTATTTAAAACCTTTCAACA
ACGGATCTCTTGGTTCCGGYATCRATGAARAACSCASCAGAAATGCGATA
CGTAATGTGAATTGCAAATTCKYGAATCATCRAKKCTTTKAACRYACA
TTGYRCCCCCTGGWATTCCSGGGGGYATGCCTGTCCGASCWMMATTGC
TGCCCTCAAGCCCRGMITTGTGTGTTGGGCCCCGTCCCCCGATCCCGGG
GGACGGGCCCRAAAGGCAGCGGGCGGCACCGCGTCCGGTCTCSASCST
ATGGGGMTTTGYCMCCCGCTCCGTARGSCCGGSCSSSSCCTGCCRATCA
ACCCCAAATTTTAAATCCAGGWTGACCTCSSATCAGGKASGGATACCCG
    
```

Fig. 1: Genetic sequencing of isolates diagnosed in the current study.

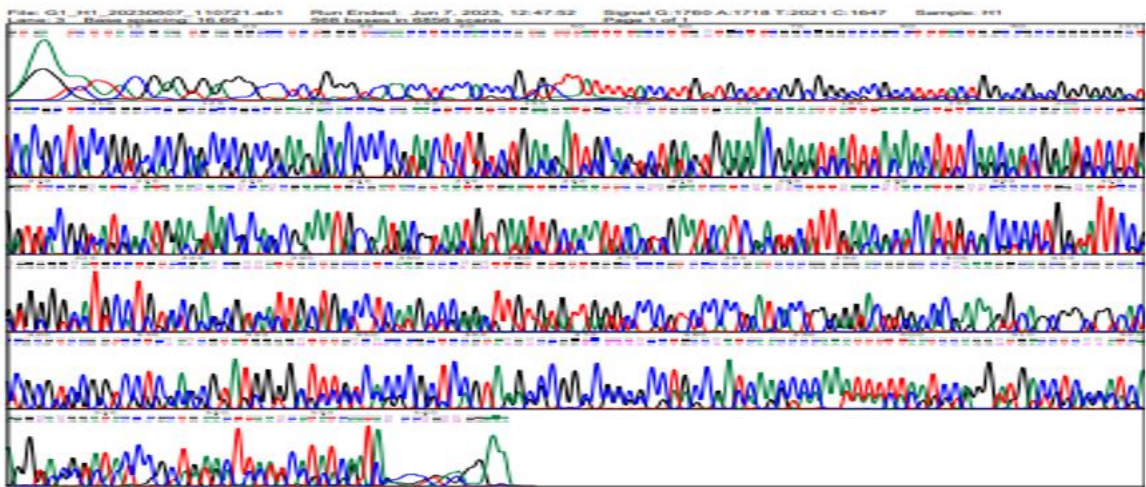


Fig. 2: The sequencing analysis image of *P. digitatum*.

select all 100 sequences selected		GenBank	GenBank	Distance	Log of Results	MSA Viewer
Description	Accession	Accession	Score	Score	Score	Accession
GTGATCTTACCGAGTGAGGGCCCTCTGGGTCCAACCTCCCACCCGTGTT...	MT175471.1	MT175471.1	100.00	100.00	100.00	MT175471.1
GTGATCTTACCGAGTGAGGGCCCTCTGGGTCCAACCTCCCACCCGTGTT...	MT175472.1	MT175472.1	100.00	100.00	100.00	MT175472.1
GTGATCTTACCGAGTGAGGGCCCTCTGGGTCCAACCTCCCACCCGTGTT...	MT175473.1	MT175473.1	100.00	100.00	100.00	MT175473.1
GTGATCTTACCGAGTGAGGGCCCTCTGGGTCCAACCTCCCACCCGTGTT...	MT175474.1	MT175474.1	100.00	100.00	100.00	MT175474.1
GTGATCTTACCGAGTGAGGGCCCTCTGGGTCCAACCTCCCACCCGTGTT...	MT175475.1	MT175475.1	100.00	100.00	100.00	MT175475.1
GTGATCTTACCGAGTGAGGGCCCTCTGGGTCCAACCTCCCACCCGTGTT...	MT175476.1	MT175476.1	100.00	100.00	100.00	MT175476.1
GTGATCTTACCGAGTGAGGGCCCTCTGGGTCCAACCTCCCACCCGTGTT...	MT175477.1	MT175477.1	100.00	100.00	100.00	MT175477.1
GTGATCTTACCGAGTGAGGGCCCTCTGGGTCCAACCTCCCACCCGTGTT...	MT175478.1	MT175478.1	100.00	100.00	100.00	MT175478.1
GTGATCTTACCGAGTGAGGGCCCTCTGGGTCCAACCTCCCACCCGTGTT...	MT175479.1	MT175479.1	100.00	100.00	100.00	MT175479.1
GTGATCTTACCGAGTGAGGGCCCTCTGGGTCCAACCTCCCACCCGTGTT...	MT175480.1	MT175480.1	100.00	100.00	100.00	MT175480.1
GTGATCTTACCGAGTGAGGGCCCTCTGGGTCCAACCTCCCACCCGTGTT...	MT175481.1	MT175481.1	100.00	100.00	100.00	MT175481.1
GTGATCTTACCGAGTGAGGGCCCTCTGGGTCCAACCTCCCACCCGTGTT...	MT175482.1	MT175482.1	100.00	100.00	100.00	MT175482.1
GTGATCTTACCGAGTGAGGGCCCTCTGGGTCCAACCTCCCACCCGTGTT...	MT175483.1	MT175483.1	100.00	100.00	100.00	MT175483.1
GTGATCTTACCGAGTGAGGGCCCTCTGGGTCCAACCTCCCACCCGTGTT...	MT175484.1	MT175484.1	100.00	100.00	100.00	MT175484.1
GTGATCTTACCGAGTGAGGGCCCTCTGGGTCCAACCTCCCACCCGTGTT...	MT175485.1	MT175485.1	100.00	100.00	100.00	MT175485.1
GTGATCTTACCGAGTGAGGGCCCTCTGGGTCCAACCTCCCACCCGTGTT...	MT175486.1	MT175486.1	100.00	100.00	100.00	MT175486.1
GTGATCTTACCGAGTGAGGGCCCTCTGGGTCCAACCTCCCACCCGTGTT...	MT175487.1	MT175487.1	100.00	100.00	100.00	MT175487.1
GTGATCTTACCGAGTGAGGGCCCTCTGGGTCCAACCTCCCACCCGTGTT...	MT175488.1	MT175488.1	100.00	100.00	100.00	MT175488.1
GTGATCTTACCGAGTGAGGGCCCTCTGGGTCCAACCTCCCACCCGTGTT...	MT175489.1	MT175489.1	100.00	100.00	100.00	MT175489.1
GTGATCTTACCGAGTGAGGGCCCTCTGGGTCCAACCTCCCACCCGTGTT...	MT175490.1	MT175490.1	100.00	100.00	100.00	MT175490.1
GTGATCTTACCGAGTGAGGGCCCTCTGGGTCCAACCTCCCACCCGTGTT...	MT175491.1	MT175491.1	100.00	100.00	100.00	MT175491.1
GTGATCTTACCGAGTGAGGGCCCTCTGGGTCCAACCTCCCACCCGTGTT...	MT175492.1	MT175492.1	100.00	100.00	100.00	MT175492.1
GTGATCTTACCGAGTGAGGGCCCTCTGGGTCCAACCTCCCACCCGTGTT...	MT175493.1	MT175493.1	100.00	100.00	100.00	MT175493.1
GTGATCTTACCGAGTGAGGGCCCTCTGGGTCCAACCTCCCACCCGTGTT...	MT175494.1	MT175494.1	100.00	100.00	100.00	MT175494.1
GTGATCTTACCGAGTGAGGGCCCTCTGGGTCCAACCTCCCACCCGTGTT...	MT175495.1	MT175495.1	100.00	100.00	100.00	MT175495.1
GTGATCTTACCGAGTGAGGGCCCTCTGGGTCCAACCTCCCACCCGTGTT...	MT175496.1	MT175496.1	100.00	100.00	100.00	MT175496.1
GTGATCTTACCGAGTGAGGGCCCTCTGGGTCCAACCTCCCACCCGTGTT...	MT175497.1	MT175497.1	100.00	100.00	100.00	MT175497.1
GTGATCTTACCGAGTGAGGGCCCTCTGGGTCCAACCTCCCACCCGTGTT...	MT175498.1	MT175498.1	100.00	100.00	100.00	MT175498.1
GTGATCTTACCGAGTGAGGGCCCTCTGGGTCCAACCTCCCACCCGTGTT...	MT175499.1	MT175499.1	100.00	100.00	100.00	MT175499.1
GTGATCTTACCGAGTGAGGGCCCTCTGGGTCCAACCTCCCACCCGTGTT...	MT175500.1	MT175500.1	100.00	100.00	100.00	MT175500.1

Fig. 3: The diagnosis of *P. digitatum*.

Synthesis of AgNPs Using *Penicillium digitatum*:

Silver nanoparticles were obtained after growing the fungus on Sabouraud Dextrose Agar medium for a week, after

which tablets with a diameter of 5 mm and more were transferred to Potato Sucrose liquid medium in a bottle of 1000 ml to ensure that bacteria did not grow. Using Watman1 filter papers the biomass was transferred to

glass containers after washing them with deionized water weighing 20 grams of biomass, then incubated in containers containing 500 ml of deionized water for 120 hours, and then the biomass was filtered using filters of size 0.4 to obtain a biomass filtrate. For mushrooms and filtrate collection. The results showed that the weights of the biomass are 80gm, respectively, and this is due to the fact that its production of biomass is very fast and the most growing, and that is a result of its high metabolic efficiency. Then it was filtered with filter papers and dried until the required tests were performed (Pranay & Archit 2013, Mirzaei *et al.*, 2019).

Characterization of Synthesized AgNPs:

Examination of structural, surface, volumetric, and optical properties of nanobodies isolated from fungi. The silver nanoparticles (Ag and Ag₂O) prepared by *Penicillium digitatum* were isolated and diagnosed microscopically and molecular for the production of silver nanoparticles and the examination of their structural, surface, volumetric and optical properties using three methods represented by the X-ray diffraction method, the electronic scanner method and the visible ray absorption spectrometry (Jihad, *et al.*, 2021). The composition of nanoparticles has been observed through a number of indicators as follows:

Structural Properties of Nanoparticles Using X-ray Diffraction Method:

Due to the fact that *Penicillium digitatum* fungal isolates gave the best results. The ability to produce nanoparticles and study the structural properties of the fungus was confirmed represented in Figure (4), where the X-ray diffraction spectrum of silver particles (Ag and Ag₂O) nanoparticles prepared by employing *Penicillium digitatum* fungi was confirmed. We note from the figure that the prepared samples show the presence of 4 diffraction peaks for

silver particles at crystal levels (220) and 3 diffraction peaks for silver oxide particles at crystal levels (220). After comparing diffraction angle values with the checklist of X-ray diffraction measurements and material ¹ diagnostics (Joint Committee on Powder Difference Standards: JCPDS cards). The measurements showed a match with the standard PDF Card: 004-0783 for silver nanoparticles (AgNPs) and the standard PDF card: 041-1104 for silver oxide nanoparticles (Ag₂O). These results are similar to the researchers' findings (Hussein, 2016; Pranay and Archit; 2013; Swathi, *et al.*, 2014; Pavani, *et al.*, 2012; Deepak, and Aruna, 2014). The X-ray spectrum also shows high-intensity diffraction peaks, a characteristic of highly crystalline materials, with a diffraction peak prevailing towards level (111), which indicates that the prepared particles possess the nanostructured characteristic. The crystallization of the silver oxide phase in the samples can be due to the synergy of the silver ions with the oxygen ions present in the solution in which the fungus grows during preparation. Table 1 shows that the values of diffraction angles, crystal plane directions, and full width are half the maximum (FWHM) and crystal volume (D) for each sample. The crystal volume (D) was calculated from the width of the diffraction curve using the FWHM-based Scherrer equation after substituting into the following equation (Adibhesami *et al.*, 2017 Ak1, 2020).

$$D = 0.9 * \frac{\lambda}{FWHM} * \cos(\theta) \dots (1)$$

Here (θ) represents the X-ray diffraction angle, (λ) represents the wavelength of the X-rays used, which is equal to (1.5406 Å). Crystal size is an important parameter as crystal sizes determine whether a material is soft (small crystals) or brittle (large crystals) (Hasoon, 2019).

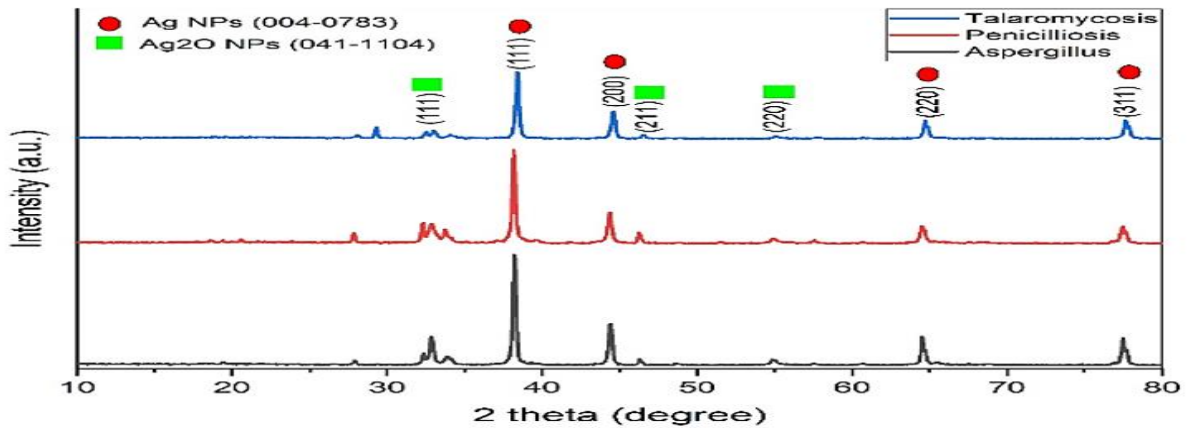


Fig. 4: X-ray diffraction spectrum of silver nanoparticles prepared by fungi.

The results confirmed that the average crystal size of the silver nanoparticles in the sample prepared by *Penicillium digitatum* was less than 100 nm, as shown in Table 1 and Figure 5. The increase in crystal

size can be attributed to the agglomeration processes experienced by nanoparticles when the density of atoms increases and thus increases their bonding ability with each other.

Table 1: X-ray diffraction coefficients of nanoparticles prepared by fungus *P. digitatum*.

Nanoparticles	2 theta (degree)	hkl (panel)	FWHM (deg)	2 theta (Rad.)	FWHM (Rad.)	D (nm)	D average (nm)
AgNPs Ag ₂ ONPs (*)	32.839	(111)*	0.3149	0.230	0.005	25.900	31.36
	38.165	(111)	0.1968	0.310	0.003	42.371	
	44.352	(200)	0.2755	0.387	0.005	31.127	
	46.243	(211)*	0.2362	0.404	0.004	36.557	
	54.931	(220)*	0.2477	0.479	0.004	36.132	
	64.542	(220)	0.3149	0.563	0.005	29.825	
	77.451	(311)	0.576	0.676	0.010	17.672	

It was noted that (Silambarasan & Abraham 2012) estimated the diameter of titanium nanoparticles manufactured by *B. cereus* bacteria at 40.71 nm using the atomic force microscope (AFM) method, while the average size and diameter of the particles manufactured by *A. flavus* were about 3574.67 and 67.46 nm respectively. (Singh & Chopade 2015, Pérez-Díaz *et al.*, 2015) shows that the average size of nanoparticles

prepared from *Penicillium digitatum* isolated from the industrial district is about 011. Nanometers and for the fungus isolated from *F. solani* from Gemen were about 8.1 nm and *P. Expansum* from the industrial district about 6 nm. The difference in diameter may be due to the different measurement methods and sources of the fungus manufactured for nanoparticles.

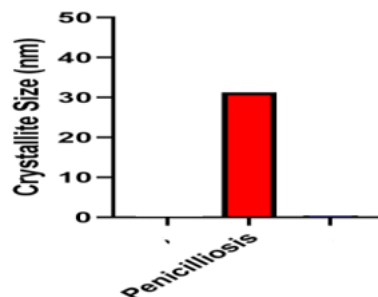


Fig. 5: Crystal Size Rate of Silver Nanoparticles Prepared by *P. digitatum*.

The Field-Emission Scanning Electron Microscopy(FESEM):

FESEM is one of the most important tools that can be employed to know the surface topography of materials within the nanoscale, as it allows knowing the shape of nanoparticles with high accuracy and at different magnifications. Figure (6) shows a general survey of the topography of silver nanoparticles (Ag and Ag₂O) prepared by using the fungus (*Penicillium digitatum*).

The results confirm that all samples show the collection of a large number of nanoparticles of different and of spherical structure, where they collectively form a nanostructured similar to cluster nanoparticles. This behavior in the formation of spherical nanoparticles or nanoclusters is one of the most important characteristics of silver nanoparticles, giving them a high surface area and the ability to penetrate the components of living cells (Bhuyar *et al.* ,2020).

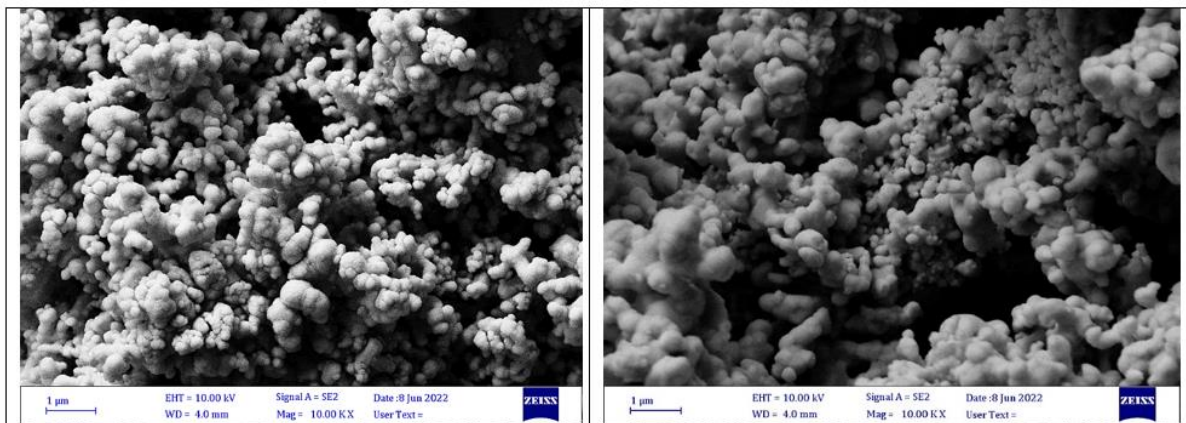


Fig.6: The morphological form of silver nanoparticles prepared by fungi *Penicillium digitatum* at the micro and nanoscale.

X-ray spectroscopy: EDS is an analytical technique used to analyze elements to find out the chemical properties of samples. Figure (7) shows the dispersion spectroscopy of silver nanoparticles (Ag and Ag₂O) prepared by using *Penicillium digitatum*. The

results show the presence of high energy peaks for silver metal and low energy peaks due to oxygen, with very high weight ratios (wt.%) for silver compared to oxygen, as shown in Table (2).

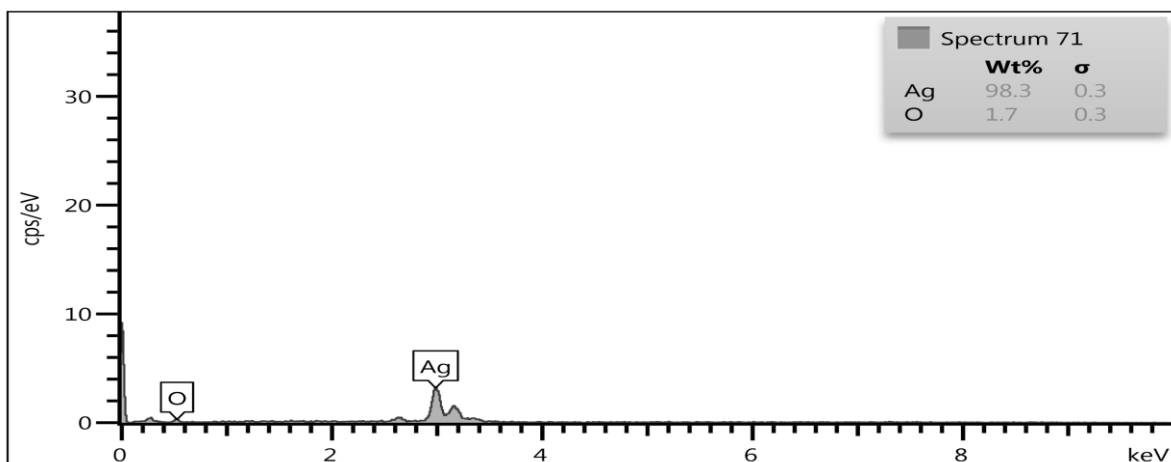


Fig. 7: The morphological form of silver nanoparticles prepared by fungi, *P. digitatum* at the micro and nanoscale.

The gravimetric results shown in Table (2), indicate conformity with the X-ray diffraction results and support a high content of pure silver compared to oxidized silver.

The results also show that the oxygen content was higher in the sample prepared by *Penicillium digitatum* compared to the rest of the samples.

Table 2: Weight ratios of silver and oxygen in each prepared sample

Samples.	Ag (wt.%)	O (wt.%)
<i>Penicillium digitatum</i>	98.3	1.7

Transmission Electron Microscope (TEM) is a very powerful tool for materials science. A beam of high-energy electrons illuminates a very thin sample and passes through it, and interactions between atoms

and electrons can be used to observe features such as crystal structure. (Crystal-structure), grain boundaries, shape and size of nanoparticles shown in Figure 8

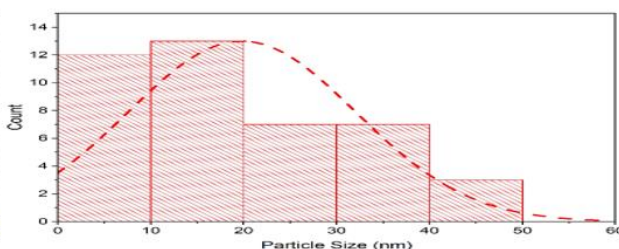
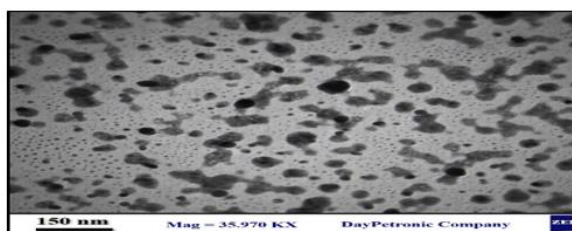


Fig.8: silver nanoparticles prepared by *P. digitatum* fungi by transmission electron microscope.

Figure 8 shows the transmitting electron microscope of silver nanoparticles (Ag and Ag₂O) prepared using *Penicillium digitatum*, fungi with a histogram for each sample. Figure 5 confirms the existence of a uniform distribution of nanostructures with particle-like shapes. Semi-spherical nanoparticles, and a peak distribution of nanoparticles at size 30 nm.

Optical Properties of Nanoparticles Using UV-Visible Light Absorption Spectroscopy Method:

Figure (9) shows the optical absorption spectrum of silver nanoparticles (Ag and Ag₂O) prepared by a single fungus using the method of absorption of ultraviolet and visible rays at a wavelength range of 250 to 650 nm, which is one of the important techniques for detecting nanostructures as a result of irritation of vibrations in plasmon

(electron or gap) at the metal surface. The results shown in Figure (6) confirm that the optical absorption spectrum shows a significant change in optical behavior when using *Penicillium digitatum*. The results indicate stability in the absorption of the spectrum in the visible region with a strong absorption edge in the ultraviolet region that begins to rise at a wavelength of 325 nm and reaches the peak absorption at a wavelength of 255 nm. This behavior can be attributed to an increase in the oxygen content in the sample that causes a decrease in surface plasmon activity and absorption in the visible region of the electromagnetic spectrum. The current results are identical to the results of the measurement of EDS and the results of the absorption spectrum at work (Gannoruwa, *et al.*, 2019, Duran, 2010).

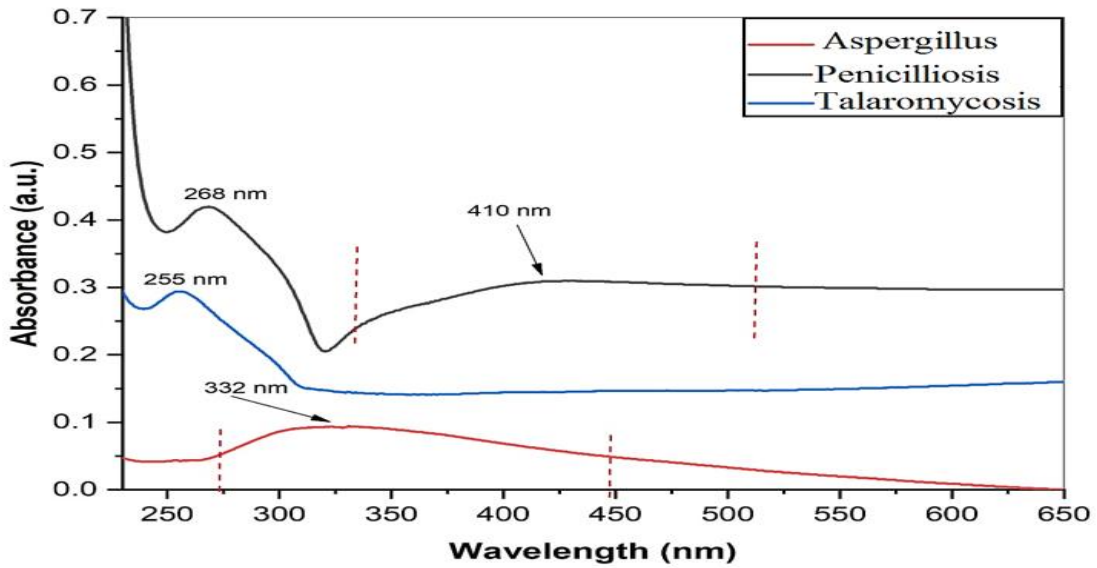


Fig. 9: Optical absorption spectrum in the ultraviolet and visible region of silver nanoparticles prepared by *Penicillium digitatum* fungi.

Effect of Silver Nanoparticles AgNPs Extracted from *P. digitatum* on Some Pathogenic Bacteria:

Effect of Silver Nanoparticles AgNPs Extracted from *P. digitatum* on *Proteus mirabilis*:

The effect of nanoparticles prepared from *Penicillium digitatum* showed that the inhibition diameter reached (22.5, 17.5) mm

respectively, with a concentration of 100% on *Proteus mirabilis* bacteria, while the inhibition diameter reached (19.5, 16.5) mm respectively, at a concentration of 50% and A is the control, while the sources of bacterial isolation and inhibition diameter reached (18.5, 15.5) mm respectively, at a concentration of 25% as shown in Table (3), Figure (10) and Figure (11).

Table 3: Effect of nanoparticles extracted from *Penicillium digitatum* fungi, in different concentrations on *Proteus mirabilis* bacteria.

Sample	Source of infection	A Control	B %10	C %25	D %50	E %100
<i>Proteus mirabilis</i> 38	Urinary tract infection	6	17	18	19	22
<i>Proteus mirabilis</i> 6	Skin Infection	6	14	15	16	17

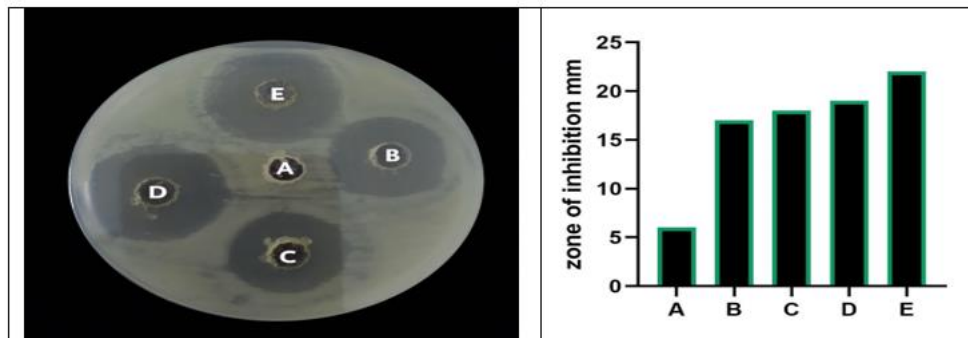


Fig. 10: Antibacterial efficacy of nanoparticle against *P. marabillus* 38. (A) control, (B) 10%, (C) 25%, (D) 50%, (E) 100%.

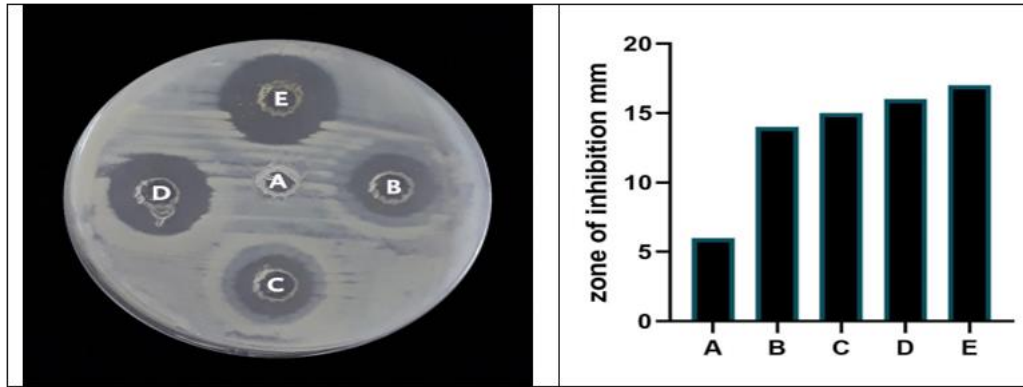


Fig. 11: Antibacterial efficacy of nanoparticle against *P. marabillus* (6). (A) control, (B) 10%, (C) 25%, (D) 50%, (E) 100%.

Effect of Silver Nanoparticles AgNPs Extracted from *P. digitatum* on *Acinetobacter baumannii*s:

The results showed the effect of different concentrations of silver nanoparticles produced from the fungi *Penicillium digitatum* on the growth of two isolates of *Acinetobacter baumannii*s. It was isolated from different skin infections and *Acinetobacter baumannii*s were isolated from respiratory infections. After that, it was diagnosed by a biochemical test, and it was used from differentiating media that distinguishes the genus *Acinetobacter* from other negative and non-fermenting lactose species, using blood agars containing the sugar Aldose, and changing the color of the medium to brown. Antibacterial efficacy of nanoparticle against *Acinetobacter baumannii*s bacteria under study shown in Table (4). The results showed that the use of nanoparticles extracted from *Penicillium digitatum* fungus at a concentration of 100% caused inhibition on *Acinetobacter* 1 and *Acinetobacter* 2, as the inhibition diameter reached (17.18) mm respectively, (Fayaz *et al.*,2010, Lara *et al.*.,2009). The inhibition diameter reached (13.12) mm respectively, when diluting 50%, but when diluting

concentrations to 25%, the inhibition diameter of bacteria reached (8) mm for each of *Acinetobacter* 1 and *Acinetobacter* 2 bacteria, as shown in Figures (14 and 15).

The results showed that when using nanoparticles isolated from *Penicillium digitatum* on *Acinetobacter* 1 and *Acinetobacter* 2 bacteria, the inhibition diameter was (19, 15) at a concentration of 100%, while the inhibition diameter decreased to (14, 14) mm for each of the two isolates at a concentration of 50%. The inhibition diameter was (8.5, 8) at a concentration of 25% for both isolates and no growth on concentrations A control. Because it does not contain silver nanoparticles as shown in Figures (12 and 13).

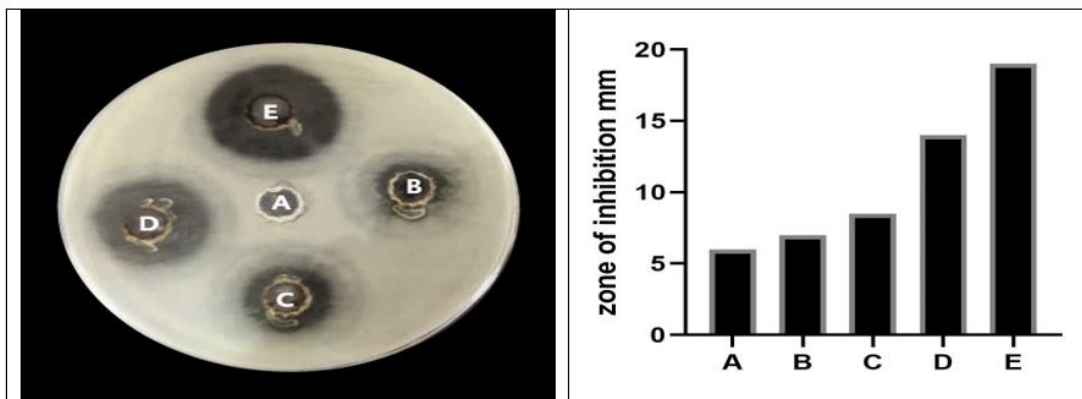
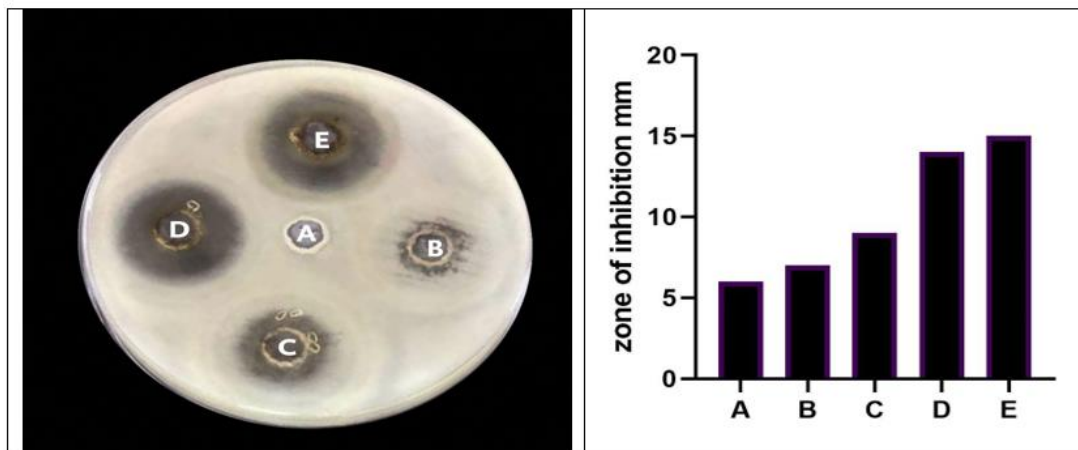
The inhibition diameter reached (13, 19) mm when testing the effect of nanoparticles produced from *Penicillium digitatum* at a concentration of 100% on the bacterial isolates *Acinetobacter* 1 and *Acinetobacter* 2 respectively. While the retarding diameter reached (9, 15) mm respectively, while the retarding diameter reached (8, 9.5) mm respectively at a concentration of 25%. As indicated in Table (4).

Table 4: Effect of nanoparticles extracted from *Pencillium digitatum* fungi. A Control B %10, C %25 . D % 50, E % 100.

Sample	Source	A Control	B %10	C %25	D %50	E %100
<i>Acinetobacter baumannii</i> 1	Skin infection	6	7	8.5	14	19
<i>Acinetobacter baumannii</i> 2	Respiratory infections	6	7	9	14	15

A. baumannii exhibits a remarkable capacity to endure adverse environmental conditions and propagate as a significant pathogenic agent. *Acinetobacter baumannii* is known to infect moist tissues, including mucous membranes and exposed areas of the skin resulting from wounds or injuries. (Hetta *et al.*, 2021, Lok *et al.*.,2006), they reported that the presence of AgNPs resulted in a decreased growth rate of *A. baumannii*. The antimicrobial and antibiofilm properties of silver nanoparticles (AgNPs) were found to be particularly effective against strains of

bacteria with lower biofilm production capabilities (Abdulbaqi *et al.*,2018). The results showed that when using nanoparticles isolated from *P. digitatum* (2) on *Acinetobacter* 1 and *Acinetobacter* 2, the inhibition diameter was (19, 15) at a concentration of 100%, while, the inhibition diameter decreased to (14, 14) mm for each of the two isolates at a concentration of 50%, while, the inhibition diameter was (8.5, 8) at a concentration of 25% for both isolates as shown in Figures (12) and Figure (13).

**Fig. 12** Antibacterial efficacy of (2) against *Acinetobacter* 1, A control, B 10%, C 25%, D 50%, E 100.**Fig. 13** :Antibacterial efficacy of *P. digitatum* against *Acinetobacter* 2, A / control, B 10%, C 25%, D 50%, E 100%.

Antibiotics Sensitivity Test:

During this test, 10 types of antibiotics were used, and the tablet method was used, with different concentrations. The antibiotics are (Eyrthromycin E), (Ceftraxone CRO), (Gentamcin GN), (Amikacin AK), (Azimac Azm) (Cefazidime CAZ), (Ampicillin AM), (Ceftaxin CTX), (Levofloxacin Lev), (Ciprofloxacin Cip). It is clear from the results (Table 5) that bacterial *P. mirabilis6* isolates are resistant to all types of antibiotics, as these are resistant to many commonly used antibiotics such as beta-

lactams, aminoglycosides, also bacteria *P. mirabilis6* resistant to all antibiotics except antibiotics Levofloxacin, as for bacteria *A.baumannii* 1. It showed high resistance to antibiotics except for Ciprofloxacin and Levofloxacin and Amikacin antibiotics. *A.baumannii* 2 bacteria resisted all types of antibiotics except Levofloxacin and Ampicillin and Cefazidime antibiotics, and the reason is due to the bacteria having different virulence factors such as biofilm and production of enzymes in addition to the presence of resistance genes. Table 5.

Table 5: Antibiotics Sensitivity Test.

Antibiotic	Cip	Lev	E	CTX	AM	CAZ	AZM	AK	GN	CRO
	5	10	15	15	10	30	10	30	10	8
<i>P. mirabilis38</i>	R	20	R	R	R	R	R	R	R	R
<i>P. mirabilis6</i>	R	R	R	R	R	R	R	R	R	R
<i>A.baumannii</i> 1	26	25	R	R	R	R	R	20	R	R
<i>A.baumannii2</i>	R	25	R	R	25	R	25	R	R	R

Eyrthromycin E), (Ceftraxone CRO), (Gentamcin GN), (Amikacin AK), (Azimac Azm) (Cefazidime CAZ), (Ampicillin AM), (Ceftaxin CTX), (Levofloxacin Lev), (Ciprofloxacin Cip). R Resistance

Conclusion

The silver nanoparticles synthesized from fungi *P. digitatum* vary in their effect against bacteria *Proteus marabilis*, *Acinetobacter baumannii*es Resistance to antibiotics.

REFERENCES

- Abdulbaqi, N. J. and Dheeb, B. I. and Irshad, R.. Expression of Biotransformation and Antioxidant Genes in the Liver of Albino Mice after Exposure to Aflatoxin B1 and an Antioxidant Sourced from Turmeric (*Curcuma longa*). (2018). *Jordan Journal of Biological Sciences*, 11(2) 89 – 93.
- Adibhesami, M., Ahmadi, M., Farshid, A. A., Sarrafzadeh-Rezaei, F., & Dalir-Naghadeh, B. (2017). Effects of silver nanoparticles on *Staphylococcus aureus* contaminated open wounds healing in mice: An experimental study. In *Veterinary Research Forum*, (Vol. 8, No. 1, p. 23). Faculty of Veterinary Medicine, Urmia University, Urmia, Iran.
- Akl, B., Nader, M., El-Saadony, M. (2020). Biosynthesis of Silver Nanoparticles by *Serratia marcescens* ssp *sakuensis* and its Antibacterial Application against some Pathogenic Bacteria. *Journal of Agricultural Chemistry and Biotechnology*, 11(1), 1-8.
- Al-Ezzy, A. I. A., Al-Azawi, S. A., & Algburi, A. (2023). Multidrug Resistant Behavior Of *Proteus mirabilis* Isolated From patients with Urinary Tract Infections. *Diyala Journal for Veterinary Sciences*, 1(1), 1-15.
- Al-Tekreeti, A. R., Al-Halbosiy, M. M. F., Dheeb, B. I., Hashim, A. J. and Al-Zuhairi, A. F. H.. Molecular identification of clinical *Candida* isolates by simple and randomly amplified polymorphic DNA-PCR. (2017). *Arabian Journal for Science and Engineering (AJSE)*, DO

- I 10.1007/s13369-017-2762-1.
- Badali, H., Cañete-Gibas, C., McCarthy, D., Patterson, H., Sanders, C., David, M. P., ... & Wiederhold, N. P. (2021). Epidemiology and antifungal susceptibilities of mucoralean fungi in clinical samples from the United States. *Journal of clinical microbiology*, 59(9), 10-1128.
- Bhuyar, P., Rahim, M. H. A., Sundararaju, S., Ramaraj, R., Maniam, G. P., & Govindan, N. (2020). Synthesis of silver nanoparticles using marine macroalgae *Padina* sp. and its antibacterial activity towards pathogenic bacteria. *Beni-Suef University Journal of Basic and Applied Sciences*, 9, 1-15.
- Dahham, M.T., Omar, A.F., Dheeb B.I. Synergistic effect of tea tree oil on fungi causing vaginal thrush in pregnant women(2019). *Journal of Biotechnology Research Center*, 13 (2)35-44.
- Duran, N.; Marcato, P. D.; Conti, R. D.; Alves, O. L.; Costa, F. M. and Brocchi, M.(2010). Potential use of Silver Nanoparticles on pathogenic bacteria, their toxicity, and possible mechanisms of action. *Journal of the Brazilian Chemical Society*, 21 (6):949-959.
- Fayaz, A.M.; Balaji, K.; Girilal, M.; Yadav, R.; Kalaichelvan, P.T. and Venketesan, R. (2010). Biogenic synthesis of silver Nanoparticles and their synergistic effect with antibiotics: A study against gram-positive and gram negative bacteria. *Nanomedicine*, 6:103–106.
- Gannoruwa, A. Ariyasinghe, B. and Bandara, J. "The mechanism and material aspects of a novel Ag₂O/TiO₂ photocatalyst active in infrared radiation for water splitting," *Catalysis Science and Technology*, vol. 6, no. 2, pp. 479-487, 2016.
- Gedefie, A., Demsis, W., Ashagrie, M., Kassa, Y., Tesfaye, M., Tilahun, M., ... & Sahle, Z. (2021). *Acinetobacter baumannii* biofilm formation and its role in disease pathogenesis: a review. *Infection and Drug Resistance*, 3711-3719.
- Hashim S. S, Mahmood Z. F, Abdulateef S. F, Dheeb B. I. Evaluation Cytotoxicity Effects of *Centaurea Cineraria* Extracts Against some of Cancer Cell Lines. *Biomedical and Pharmacology Journal*, 2023;16(1).
- Hetta, H. F., Al-Kadmy, I. M., Khazaal, S. S., Abbas, S., Suhail, A., El-Mokhtar, M. A., ... & Algammal, A. M. (2021). Antibiofilm and antivirulence potential of silver nanoparticles against multidrug-resistant *Acinetobacter baumannii*. *Scientific reports*, 11(1), 10751.
- Hezam, A. M., Yousif, M. G., & Mohammed, G. J. (2023, July). Detection of Auxotroph's Methionine *Proteus Mirabilis* from Different Clinical Sources. In IOP Conference Series: *Earth and Environmental Science*, (Vol. 1215, No. 1, p. 012065). IOP Publishing.
- Hussain, A.F., Sulaiman, G.M., Dheeb, B.I., Hashim, A.J., Histopathological changes and expression of transforming growth factor beta (TGF-β3) in mice exposed to gliotoxin.(2018). *Journal of K S U Science*, 27, 193–197.12.
- Hussein, H.S., Dheeb B.I., Hamada,T.A.. Studying the candida resistance and sensitivity for some antifungals (2019). *Journal of Biotechnology Research Center*, 13 (2)25-34.
- Jihad, M. A., Noori, F., Jabir, M. S., Albukhaty, S., AlMalki, F. A., and Alyamani, A. A. (2021). Polyethylene Glycol Functionalized Graphene Oxide Nanoparticles Loaded with *Nigella sativa* Extract: A Smart Antibacterial Therapeutic Drug Delivery System. *Molecules*, 26(11), 3067.
- Jillwin, J., Rudramurthy, S. M., Singh, S., Bal, A., Das, A., Radotra, B., ... & Chakrabarti, A. (2021). Molecular

- identification of pathogenic fungi in formalin-fixed and paraffin-embedded tissues. *Journal of Medical Microbiology*, 70(2), 001282.
- Khashan, K. S., Abdulameer, F. A., Jabir, M. S., Hadi, A. A., and Sulaiman, G. M. (2020). Anticancer activity and toxicity of carbon nanoparticles produced by pulsed laser ablation of graphite in water. *Advances in Natural Sciences: Nanoscience and Nanotechnology*, 11(3)
- Khashan, K. S., Badr, B. A., Sulaiman, G. M., Jabir, M. S., and Hussain, S. A. (2021). Antibacterial activity of Zinc Oxide nanostructured materials synthesis by laser ablation method. In *Journal of Physics: Conference series*, Vol. 1795, No. 1, p. 012040.
- Khazaal, S. S., Al-Kadmy, I. M., & Aziz, S. N. (2020). Mechanism of pathogenesis in multidrug resistant *Acinetobacter baumannii* isolated from intensive care unit. *Gene Reports*, 18, 100557.
- Khezerlou, A., Alizadeh-Sani, M., Azizi-Lalabadi, M., & Ehsani, A. (2018). Nanoparticles and their antimicrobial properties against pathogens including bacteria, fungi, parasites and viruses. *Microbial pathogenesis*, 123, 505-526.
- Lara, H. H., Ayala-Núñez, N. V., Ixtapan Turrent, L. del C., & Rodríguez Padilla, C. (2009). Bactericidal effect of silver nanoparticles against multidrug-resistant bacteria. *World Journal of Microbiology and Biotechnology*, 26(4), 615-621.
- Lok, C.N.; Ho, C.M.; Chen, R.; He, Q.Y.; Yu, W.Y.; Sun, H.; Tam, P.K.; Chiu, J. F. and Chen, C.M. (2006). Proteomic Analysis of the mode of antibacterial action of silver nanoparticles. *Journal of Proteome Research*, 5:916-924.
- Mirzaei, A., Habibi, M., Bouzari, S., & Asadi Karam, M. R. (2019). Characterization of antibiotic-susceptibility patterns, virulence factor profiles and clonal relatedness in *Proteus mirabilis* isolates from patients with urinary tract infection in Iran. *Infection and drug resistance*, 3967-3979.
- Mittal, A. K., Bhaumik, J., Kumar, S., & Banerjee, U. C. (2014). Biosynthesis of silver nanoparticles: elucidation of prospective mechanism and therapeutic potential. *Journal of colloid and interface science*, 415, 39-47.
- Nath, D., Singh, F., & Das, R. (2020). X-ray diffraction analysis by Williamson-Hall, Halder-Wagner and size-strain plot methods of CdSe nanoparticles- a comparative study. *Materials Chemistry and Physics*, 239, 122021.
- Nouri, M. A., Al-Halbosiy, M. M. F., Dheeb, B. I. and Hashim, A. J. Cytotoxicity and genotoxicity of gliotoxin on human lymphocytes in vitro. (2015). *Journal of K S U – Science*, 27, 193-197.
- Panacek, A.; Kvitek, L.; Pucek, R.; Kolar, M.; Vecerova, R.; Pizurova, N.; Sharma, V. K.; Nevecna, T. and Zboril, R. (2006). Silver colloid nanoparticles: synthesis, characterization, and their antibacterial activity. *The Journal of Physical Chemistry B*, 110(33): 16248-53.
- Pérez-Díaz, M. A., Boegli, L., James, G., Velasquillo, C., Sánchez-Sánchez, R., Martínez-Martínez, R. E., ... & Martínez-Gutierrez, F. (2015). Silver nanoparticles with antimicrobial activities against *Streptococcus mutans* and their cytotoxic effect. *Materials Science and Engineering: C*, 55, 360-366.
- Pranay, J., & Archit, S. (2013). Antimicrobial activity of silver nanoparticles synthesized from *Aspergillus* species against common oral pathogens. Department of Biotechnology, University Institute of Engineering and Technology, Kurukshetra

- University, Kurukshetra, India. *Journal of Chemical and Pharmaceutical Research*, 5(2), 14-17.
- Rahi, D. K., & Parmar, A. S. (2014). Mycosynthesis of silver nanoparticles by an endophytic *Penicillium* species of Aloe vera root, evaluation of their antibacterial and antibiotic enhancing activity. *International Journal of Nanomaterials Biostructures*, 4 (3): 46, 51.
- Rassin, N. K., Nemat J. A, Dheeb, B. I. Molecular Identification of *Aspergillus fumigatus* Using ISSR and RAPD Markers. *Iraqi Journal of Science*, (2015). 56 (4A), 2788-2797.
- Salomoni, R, Léo, P, Montemor, AF, Rinaldi, BG and MFA Rodrigues (2017). Antibacterial effect of silver nanoparticles in *Pseudomonas aeruginosa*, *Nanotechnology, Science and Applications*, 10:, 115-121.
- Silambarasan, S., & Abraham, J. (2012). Biosynthesis of silver nanoparticles using the bacteria *Bacillus cereus* and their antimicrobial property. *International Journal of Pharmacy and Pharmaceutical Sciences*, 4(Suppl 1), 536-40.
- Singh, R., Shedbalkar, U. U., Wadhvani, S. A., & Chopade, B. A. (2015). Bacteriogenic silver nanoparticles: synthesis, mechanism, and applications. *Applied microbiology and biotechnology*, 99, 4579-4593.
- Swathi G, A Sridevil, A Sandya², B Praveen¹, G Narasimha¹ (2014). Biosynthesis, characterization and antibacterial activity of silver nanoparticles by soil fungi *Penicillium* sps. *International Journal of Drug Delivery*, 6: 165-171.